General and specific patterns of cortical gene expression as substrates of complex cognitive functioning

Joanna E. Moodie✉[1,2], Sarah E. Harris[1], Mat A. Harris[1], Colin R. Buchanan[1,2], Gail Davies [1], Adele Taylor[1], Paul Redmond[1], David Liewald[1], Maria del C Valdés Hernández[1,3], Susan Shenkin[1,3,4], Tom C. Russ[1,3,5], Susana Muñoz Maniega[1,3], Michelle Luciano[1], Janie Corley[1], Aleks Stolicyn[3], Xueyi Shen[3], Douglas Steele[2], Gordon Waiter[2], Anca Sandu-Giuraniuc[2], Mark E. Bastin[1,3], Joanna M. Wardlaw[1,3], Andrew McIntosh[3], Heather Whalley[3], Elliot M. Tucker-Drob[6], Ian J. Deary[1], & Simon R. Cox✉[1,2]

[1] Lothian Birth Cohorts, Department of Psychology, The University of Edinburgh, UK,

[2] Scottish Imaging Network, A Platform for Scientific Excellence (SINAPSE) Collaboration, Edinburgh, UK

[3] Division of Psychiatry, Centre for Clinical Brain Sciences, University of Edinburgh, UK

[4] Ageing and Health Research Group, Usher Institute, University of Edinburgh, UK

[5]Alzheimer Scotland Dementia Research Centre, University of Edinburgh, UK

[6] Department of Psychology, University of Texas, Austin, Texas 78712-0187, USA.

✉ Corresponding authors:

Joanna E. Moodie, Lothian Birth Cohorts, Department of Psychology, The University of Edinburgh, Edinburgh EH8 9JZ, UK. Email: Joanna.moodie@ed.ac.uk

Simon R. Cox, Lothian Birth Cohorts, Department of Psychology, The University of Edinburgh, Edinburgh EH8 9JZ, UK. Email: simon.cox@ed.ac.uk.

Acknowledgements

We thank the participants of the three cohorts (UKB, Generation Scotland (STRADL) and LBC1936) for their participation and the research teams for their work in collecting, processing and giving access to these data for analysis. We are also thankful the brain donors to the Allen Human Brain Atlas, BrainSpan Atlas and Human Brain Transcriptome Project, and to the people who collected and processed the data and made it openly available.

SRC and JEM were supported by a Sir Henry Dale Fellowship, jointly funded by the Wellcome Trust and the Royal Society [221890/Z/20/Z]. For the purpose of open access, the author has applied a CC-BY public copyright licence to any Author Accepted Manuscript version arising from this submission. The LBC1936, supported by the BBSRC & ESRC [BB/W008793/1], Age UK [Disconnected Mind project], the Medical Research Council (MR/M01311/1; MR/K026992/1), the US National Institutes of Health [R01AG054628] and the University of Edinburgh. CRB, MEB, EMT-D, IJD and SRC were supported by a National Institutes of Health (NIH) research grant R01AG054628. TCR is a member of the Alzheimer Scotland Dementia Research Centre funded by Alzheimer Scotland. MCVH is funded by The Row Fogo Charitable Trust Centre for Research into Aging and the Brain (BRO-D.FID3668413).AS was funded as part of the STRADL study (Wellcome Trust reference 104036/Z/14/Z) and indirectly through the Lister Institute of Preventive Medicine research award for Prof. Daniel Smith (ref. 173096).

Conflicts of interest

None

Abstract

Gene expression varies across the brain. This spatial patterning denotes specialised support for particular brain functions. However, general rules may govern shared spatial fluctuations in expression across the genome. Such information would offer insights into the molecular characteristics of brain areas supporting, for example, complex cognitive functions. We find that the region-to-region variation in cortical expression profiles of 8235 genes covary across two major dimensions: cell-signalling/modification and transcription factors. These patterns are validated out-of-sample and across different data processing choices. Brain regions most strongly implicated in general cognitive ability (*g*; meta-analytic N = 40,929) have greater balance between downregulation and upregulation of both major components. We identify a further 34 genes as candidate substrates of *g*. The results provide insights into the cortical organisation of gene expression and its association with individual differences in cognitive functioning.

Introduction

In any given cell, genes that are required for that cell's function are expressed. Therefore, it is tenable that observed regional variations in the expression of genes across the brain reflect location-pertinent cellular processes critical for functioning. Information about regional gene expression profiles across the cerebral cortex has been recently used to infer substrates of brain development, maintenance and health (1,2,3,4). This is achieved by comparing the spatial agreement between the brain regional expression profiles of individual genes or gene sets with the brain regional associations with a phenotype of interest. For example, which specific genes or gene sets are more highly expressed in brain regions that are most strongly related to a particular phenotype of interest (5)? This approach, while powerful, potentially suffers from confounding by association. That is, for example, the expression of an individual gene might show a correlation with a phenotype because it reflects general rules that govern the spatial variation in the expression of very many genes over the brain's cortex, rather than something unique to the specific gene in question. There are general dimensions of spatial variation in gene expression covariance across the human body (6), and within multiple organs (7). This includes across the human cortex (8), where general dimensions of gene expression have previously been linked to in-vivo MRI estimates of cortical structural anatomy (9), and to functional MRI-derived neurocognitive associations (10,11). It is therefore critical to control for general dimensions along which regional variation in gene expression covary when seeking gene-specific associations. Because much of our information on gene expression patterns in the brain (with sufficient regional fidelity for these questions) comes from relatively few donors, it is also critical to seek out-of-sample replication. Here, we unite micro- (gene expression) and macro-level (morphometry) information about the brain, to elucidate the underlying molecular neurobiology of complex cognitive functioning.

General cognitive functioning, or '*g*', is a robust and exceptionally-well-replicated index of individual differences in cognitive functioning, capturing variance in reasoning, planning, problem-solving, some aspects of memory, processing speed and abstract thinking (12,13). It is associated with educational attainments (14), life achievements (15), health (16). and lifespan(17,18). Regions of the brain proposed to support general cognitive functioning, or '*g*' (and which relate to individual differences therein), have

been identified via an array of methods including resting state fMRI (19), structural and functional connectivity (20), lesion studies (21), post mortem brain studies (22), and genetic information (23). These brain regions overlap substantially with those associated with other summary cognitive constructs, such as executive functioning (24). Macrostructural cortical measures provide some convergent evidence for a specific patterning of brain regional *g*-correlates, particularly highlighting parieto-frontal regions (25,26). However, debate remains about the loci of *g*'s cortical correlates, for which large multi-cohort analyses are required (27). Specifically, there is uncertainty in how much overlap there is in the spatial patterns of *g* associations with cortical thickness and surface area, measures which are largely phenotypically and genetically distinct (28,29,30,31).

Here, we combine i) *post mortem* gene expression data and ii) the largest meta-analysis of the cortico-macrostructural correlates (*in vivo* MRI; cortical volume, surface area and thickness) of individual differences in cognitive ability to-date. Both are available at the same level of granularity with respect to brain regions, allowing us to quantitatively assess spatial associations between cortical gene expression and general cognitive function. Therefore, we can ask this new question: is there an association between variation in gene expression across different brain areas and how strongly brain structural measures are associated with cognitive functioning in those same brain regions? I.e. does the brain regional map of gene expression resemble the brain regional map of brain structure-cognitive function correlations?

In contrast to prior work looking at the cortical expression patterns of single candidate genes or gene types, we discover that the expression of 8235 genes varies together in a highly synchronised fashion across the cerebral cortex. Two major components account for the majority (49.4%) of the variance in regional gene expression profiles, representing a cell-signalling/modifications axis and a transcription factors axis. We address the potential limitations of having only N = 6 tissue donors and one regional sampling approach: the dimensions of gene expression are validated in two independent gene expression atlases (N = 5, N = 11 tissue donors), and are not driven by a small number of individual outlier regions. Similarly, our meta-analysis of associations between *g* and regional cortical morphometry (volume, surface area, thickness), across 3 cohorts (total N = 40,929), shows good cross-cohort consistency in regional mapping.

The patterning of *g*-associations with brain structural measures across the cortex are associated with both of the identified gene expression components, with medium-to-large effect sizes for *g*-volume and *g*-surface area associations but weaker ones for *g*-thickness. We further identify 34 single genes whose expression patterns are individually associated with *g*-cortical profiles beyond the two major dimensions of cortical gene expression. Thus, this study provides unprecedented clarity on the patterning and replicability of the brain-macrostructural correlates of cognitive ability differences, and identifies novel global and specific molecular processes that might govern them.

Methods and materials

Gene expression method

The Allen Human Brain Atlas is a high-resolution mapping of cortical gene expression for N = 6 donors (5 male, 1 female, age M = 42.50 years, SD = 13.38 years, range = 24-57 years). The complete microarray data from a custom-designed Agilent array for all 6 donors are openly available for download. French and Paus(53) summarised these data to the Desikan-Killiany cortical atlas. To briefly summarise their method (for more information, refer to the original paper and *Table S6*), gene expression values were averaged across multiple probes. Each of the 3702 brain samples was assigned to one of the 68 Desikan-Killany regions based on their MNI coordinates, and then gene expression values were averaged per region, resulting in an expression value for each gene for each region. These between-donor median expression values are publicly available (32). French and Paus also provide a method of quality control for between-donor consistency in regional gene expression profiles (53). In this method, profiles with Spearman's $\rho > 0.446$ (equivalent to one-sided $p < .05$) between the average of donor-to-median left hemisphere profile correlations are considered to have high between-donor consistency. This method results in the retention of 8325 out of 20737 genes.

The right hemisphere expression data are based on a maximum of N = 2 donors, compared to a maximum of N = 6 donors for the left hemisphere. The number of samples per region is lower in the in right hemisphere (M = 12.59, SD = 8.90, range 2-34) than the left hemisphere (M = 37.32, SD = 24.37, range = 6-100). Further details of the number of samples and donors per region are in *Table S2*. The donor-level expression data are not available, so in the present study the 8235 genes that passed the quality control protocol

in the left hemisphere were also analysed for the right. There is a strong correlation between the expression values of individual genes between hemispheres (r = 0.997, p < 2.2e-16) suggesting that, at the hemisphere level, the relative expression values for the 8235 genes were not affected by the sampling differences between the two hemispheres.

We conducted PCA on the median gene expression values of 8235 genes across 68 cortical regions – rows = cortical regions (in place of participants in a traditional PCA) and columns = genes. We performed extensive checks for the validity of the first two components – these are detailed in the Results section.

In the raw data, the right hemisphere has lower average expression values than the left hemisphere (right: M = 6.035, SD = 2.343, left: M = 6.091, SD = 2.368), t(58.345) = 6.490, p = 2.051e-08), an artefact of there being a maximum of N = 2 donors for the right hemisphere compared to a maximum of N = 6 donors for the left. This artefact creates a clear hemisphere difference centred around zero in component scores for both components: Component 1: t(65.931 = 7.794), p = 6.218e-11, *M left* = -0.687 (SD = 0.715), *M right* = 0.687 (SD = 0.739), Component 2: t(65.931) = -5.315, p = 1.388e-06, *M left* = -0.543 (SD = 0.798), *M right* = 0.543 (SD = 0.886). However, there was a strong interhemispheric correlation in scores between the 34 paired regions for both Component 1 (r = 0.815, p = 4.411e-09) and Component 2 (r = 0.725, p = 1.25e-06).

To confirm it was appropriate to treat these hemispheric differences as an artefact of the data, and thus scale the component scores in each hemisphere, we looked to the Kang et al. (33) dataset. In this dataset, there was a more even number of donors per hemisphere (left hemisphere M = 9.55, SD = 1.04 donors per region, right hemisphere region M = 7.19, SD = 0.60 donors per region), and there was no difference in means expression values per hemisphere t(19.344) = -0.852, p = .405, *M left* = 7.521 (SD = 1.944), *M right* = 7.535 (SD = 1.943). For the rotated scores of PC1 (which had a factor congruence of 0.96 with the French and Paus expression matrix), scores were comparable between hemispheres t(19.997) = -0.265, p = .794. Therefore, we deemed it appropriate to scale the component scores separately for each hemisphere in the current dataset.

124 Statistical overrepresentation analysis

125 To assist with interpretation of the two identified major components of gene expression,
126 PANTHER's protein analysis and GO-Slim molecular, biological and cellular (version 16.0,
127 released 2020-12-01) terms were analysed. All genes included in the PCA were submitted
128 as a reference set for the statistical overrepresentation analysis and 7389 out of 8235
129 (89%) genes were available in PANTHER. Fisher's exact test and FDR correction were
130 used, and four subsets of genes were tested for statistical overrepresentation:
131 Component 1 loadings < -0.3 (total N = 3371, available N = 3099, 92%) and loadings > 0.3
132 (total N = 2093, available N = 2000, 96%); and Component 2 loadings < -0.3 (total N =
133 3477, available N = 3234, 93%) and loadings > 0.3 (total N = 1706, available N = 1551,
134 91%).

135 The statistical overrepresentation results are provided in full in a supplementary data
136 file. Some genes have absolute loadings > 0.3 on both components (N = 3026, 36.75%).
137 There are also a number of genes that had absolute loadings > 0.3 only on either
138 Component 1 (N = 2438, 29.61%) or Component 2 (N = 2157, 26.19%). N = 614 genes
139 (7.46%) did not load with an absolute > 0.3 on either component, and all statistical
140 overrepresentation tests for this set were null.

141 For the two components, a gene set enrichment analysis was run in FUMA (Functional
142 Mapping and Annotation of Genome-Wide Association Studies, https://fuma.ctglab.nl/).
143 Hypergeometric tests were performed to test if genes of interest were overrepresented
144 in any of the pre-defined gene sets (those with absolute loadings > 0.3 on each
145 component), with the 8235 genes as a background set. No significant ($\alpha < .05$) gene sets
146 were obtained from the reported genes in the GWAS catalog.

147 **g ~ cortical morphometry associations meta-analysis method**

148 Cohorts

149 The UK Biobank (UKB, http://www.ukbiobank.ac.uk,34) holds data from ~500,000
150 participants, and for ~40,000 at wave 2 of data collection, data includes head MRI scans
151 and cognitive test data. In the current study, we did not include participants if their
152 medical history, taken by a nurse at the data collection appointment, recorded a diagnosis

of e.g. dementia, Parkinson's disease, stroke, other chronic degenerative neurological problems or other demyelinating conditions, including multiple sclerosis and Guillain–Barré syndrome, and brain cancer or injury (a full list of exclusion criteria is listed in *Table S10*). After these exclusions, the final study included *N* = 39,250 participants (53% female), age *M* = 63.91 years (*SD* =7.67 years) , range = 44-83 years. The UKB was given ethical approval by the NHS National Research Ethics Service North West (reference 11/NW/0382). The current analyses were conducted under UKB application number 10279. All participants provided informed consent. More information on the consent procedure can be found at https://biobank.ctsu.ox.ac.uk/crystal/label.cgi?id=100023.

STRADL is a population-based study, developed from the Generation Scotland Scottish Family Health Study. Participants who had taken part in the Generation Scotland Scottish Family Health Study were invited back to take part in this additional study, which was initially designed to study major depressive disorder, although participants were not selected based on the presence of depression (35) https://www.research.ed.ac.uk/en/datasets/stratifying-resilience-and-depression-longitudinally-stradl-a-dep. Data are available for *N* = 1188 participants. The current sample includes *N* = 1043 participants, for whom both MRI head scans and cognitive data are available (60% female), age *M* = 59.29 years (*SD* = 10.12 years), range = 26-84 years. STRADL received ethical approval from the NHS Tayside Research ethics committee (reference 14/SS/0039), and all participants provided written informed consent.

The LBC1936 is a longitudinal study of a sample of community-dwelling older adults most of whom took part in the Scottish Mental Survey of 1947 at ~11 years old, and who volunteered to participate in this cohort study at ~70 years old (36,37) https://www.ed.ac.uk/lothian-birth-cohorts. The current analysis includes data from the second wave of data collection, which is the first wave at which head MRI scans are available, in addition to cognitive tests. In total, 731 participants agreed to MRI scanning. After image processing, data were available from *N* = 636 participants (47% female), age *M* = 72.67 years, *SD* = 0.41 years, range = 70–74 years. The LBC1936 study was given ethical approval by the Multi-Centre Research Ethics Committee for Scotland, (MREC/01/0/56), the Lothian Research Ethics Committee (LREC/2003/2/29) and the Scotland A Research Ethics Committee (07/MRE00/58). All participants gave written consent before cognitive and MRI measurements were collected.

185 MRI protocols

186 Detailed information for MRI protocols in all three cohorts are reported elsewhere: UKB
187 (38), LBC1936 (39) and STRADL40, but are briefly summarised here. In the present
188 sample, UKB participants attended one of four testing sites: Cheadle (*N* = 23591, 60%),
189 Reading (*N* = 5670, 14%), Newcastle (*N* = 9938, 25%), and Bristol (*N* = 51, 0.13%).The
190 same type of scanner was used in all four testing sites, a 3T Siemens Skyra, with a 32-
191 channel Siemens head radiofrequency coil. The UKB MRI protocol includes various MRI
192 acquisitions (more details available here
193 https://www.fmrib.ox.ac.uk/ukbiobank/protocol/V4_23092014.pdf) but relevant to this
194 work are the T1-weighted MPRAGE and T2-FLAIR volumes. For T1-weighted images,
195 208 sagittal slices were acquired with a field view of 256 mm and a matrix size of 256 x
196 256 pixels, giving a resolution of 1 x 1 x 1 $mm^{3.}$ The repetition time was 3.15 ms and the
197 echo time was 1.37 ms.

198 STRADL had 2 testing sites: Aberdeen (in the present sample, *N* = 528, 51%) and Dundee
199 (*N* = 515, 49%). Detailed information about the STRADL structural image acquisitions are
200 available here https://wellcomeopenresearch.org/articles/4-185. For the current analysis,
201 we used the T1-weighted fast gradient echo with magnetisation preparation volume
202 sequence. The Aberdeen site used a 3T Philips Achieva TX-series MRI system (Philips
203 Healthcare, Best, Netherlands) with a 32-channel phased-array head coil and a back
204 facing mirror (software version 5.1.7; gradients with maximum amplitude 80 mT/m
205 and maximum slew rate 100 T/m/s). For T1-weighted images, 160 sagittal slices were
206 acquired with a field of view of 240 mm and a matrix size of 240 x 240 pixels, giving a
207 resolution of 1 x 1 x 1 mm^3. Repetition time was 8.2 ms, echo time was 3.8 ms and
208 inversion time was 1031 ms. In Dundee, the scanner was a Siemens 3T Prisma-FIT
209 (Siemens, Erlangen, Germany) with 20 channel head and neck phased array coil and a
210 back facing mirror (Syngo E11, gradient with max amplitude 80 mT/m and maximum
211 slew rate 200 T/m/s). For T1-weighted images 208 sagittal slices were acquired with a
212 field of view of 256 mm and matrix size 256 x 256 pixels giving a resolution of 1 x 1 x 1
213 mm^3. Repetition time was 6.80 ms, echo time was 2.62 ms, and inversion time was 900
214 ms.

All LBC1936 participants were scanned in the same scanner at the Brain Research Imaging Centre, Western General Hospital, Edinburgh, using a GE Signa LX 1.5T Horizon HDx clinical scanner (General Electric, Milwaukee, WI) with a manufacturer supplied 8-channel phased array head coil. More information on the structural image acquisitions for the LBC1936 cohort is available in (39). For T1-weighted images (3D IR-Prep FSPGR), 160 coronal slices were acquired, with a field of view of 256 mm and a matrix size of 192 x 192 pixels giving a resolution of 1 x 1 x 1.3 mm^3. The repetition time was 10 ms, echo time was 4 ms and inversion time was 500 ms.

For all cohorts, the FreeSurfer image analysis suite (http://surfer.nmr.mgh.harvard.edu/) was used for cortical reconstruction and volumetric segmentation. The Desikan-Killany atlas parcellation yields 34 paired regional measures in left and right cortical hemispheres (41). Different versions of FreeSurfer were used in the three cohorts (UKB = v6.0, STRADL = v5.3, LBC1936 = v5.1), and only for UKB were T2-FLAIR volumes used to improve the pial surface reconstruction. The LBC1936 and STRADL parcellations have previously undergone thorough quality control, with manual editing to rectify any issues. Manual edits were performed to ensure correct skull stripping, tissue identification and positioning of cortical regional boundary lines. The UKB regional data were extracted from the aparc.stats files and these parcellations have not been manually or automatically edited. For the current study, UKB values more than 4 standard deviations from the mean for any individual regional measure were excluded (UKB M = 24.28, SD = 19.41, range = 0–104 participants per region). For UKB and STRADL cohorts, cognitive and MRI data were collected on the same day, but in LBC1936, there was a slight delay between the two testing sessions (M =65.08, SD = 37.77 days). Raw values are plotted for mean volume, surface area and thickness by age and cohort in *Figure S3*, and for each region in *Figures S4-10*.

240 Cognitive Tests

241 All three cohorts have collected data across several cognitive tests, covering several
242 cognitive domains, which enables the estimation of a latent factor of general cognitive
243 ability *(g)*. The cognitive tests in each cohort have been described in detail elsewhere:
244 UKB (42), STRADL (43), LBC1936 (36,44,45). The measures used in the present study
245 are summarised in *Tables* S11-S11.

246 A latent factor of *g* was estimated for each cohort, using all available cognitive tests, using
247 confirmatory factor analysis in a structural equation modelling framework. Each
248 individual test was corrected for age and sex. Latent *g* model fits were assessed using the
249 following fit indices: Comparative Fit Index (CFI), Tucker Lewis Index (TLI), Root Mean
250 Square Error of Approximation (RMSEA), and the Root Mean Square Residual (SRMR)
251 (for model fits, see *Table S18*). For the LBC1936, *g* has previously been modelled with a
252 hierarchical confirmatory factor analysis approach, to incorporate defined cognitive
253 domains (46,47). Here, in keeping with these previous models, within-domain residual
254 covariances were added for four cognitive domains (Visuospatial skills, Crystalised
255 ability, Verbal memory and Processing speed). Results of the *g* measurement models are
256 summarised in *Tables S14-S17,* and *Figure S2*. For all cohorts, all estimated paths to latent
257 *g* were statistically significant with all $p < .001$.

258 The latent *g* scores were extracted for all participants. Those for UKB were multiplied by
259 -1 so a higher score reflected better cognitive performance, to match scores from STRADL
260 and LBC1936. Then, for each cohort, a standardised β was estimated between *g* and three
261 measures of cortical morphometry (volume, surface area and thickness) for each of the
262 68 regions. Cortical measures were controlled by age, sex head position in the scanner (X,
263 Y and Z coordinates), testing site (for UKB and STRADL) and lag between cognitive and
264 MRI appointments (for LBC1936). The resulting standardised β estimates for each region
265 and each measure were meta-analysed between the three cohorts (68 regions x 3
266 measures = 204 random effects meta-analyses). The full results of these meta-analyses
267 are in *Tables S14-17.*

268 Although we controlled for age for the *g*-cortical morphometry associations within each
269 cohort, each cohort had different age ranges (with the LBC1936 having a notably narrow
270 age-range of 70-74 years old), and it is possible this might affect the associations.

271 Therefore, we also tested for mean age moderation effects on meta-analytic estimates,
272 and none were significant after FDR correction (all $Q > .4$), see *Tables S22-S24*.

273 Additional analyses

274 In addition to the main analyses, which focus on *g*-associations with general and specific
275 gene expression profiles, we also ran a parallel supplementary analysis simply on the
276 regional morphometry means (see *Supplementary Text 1*).

277 **Analysis software**

278 Most analyses were conducted in R 4.0.2. (R Core Team, 2020). The psych package was
279 used for PCAs (48), the core R stats package was used for the Kruskal-Wallis tests, the
280 FSA package (49) was used for Dunn's Kruskal-Wallis multiple comparisons, and the
281 metafor (50) package was used for the meta-analyses. All structural equation models
282 were estimated in lavaan (51) with the full information maximum likelihood method. GO
283 term analyses were conducted at http://geneontology.org/, which is powered by PANTHER
284 52. FUMA https://fuma.ctglab.nl/ was used for gene set enrichment analysis for the two
285 components, and to look up previous GWAS associations with allelic status of the specific
286 individual genes-*g* associations.

287 **Data Availability**

288 All UKB data analysed herein (including IDPs) were provided under project reference
289 10279. A guide to access UKB data is available from http://www.ukbiobank.ac.uk/register-
290 apply/. To access data from the STratifying Resilience and Depression Longitudinally
291 (STRADL) study, which is part of the Generation Scotland study, see
292 https://www.research.ed.ac.uk/en/datasets/stratifyin *g*-resilience-and-depression-
293 longitudinally-stradl-a-dep, and to access the Lothian Birth Cohort data, see
294 https://www.ed.ac.uk/lothian-birth-cohorts/data-access-collaboration.

295 **Results**

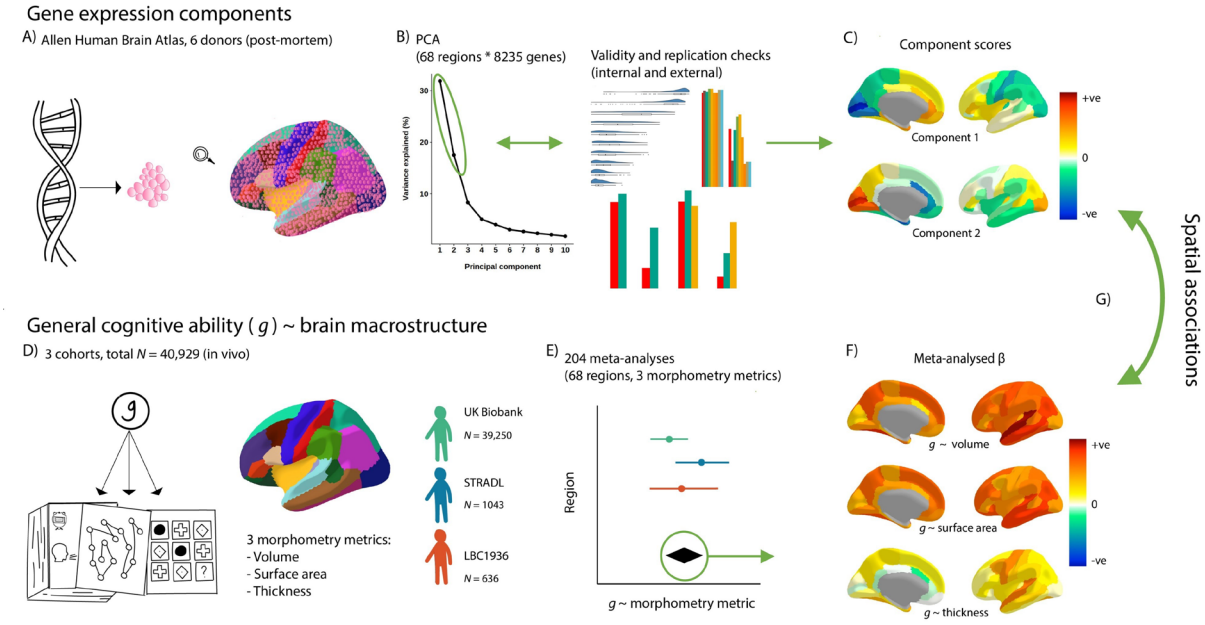

296

297 *Figure 1* An illustration of the analytic framework.

298 *Figure 1 note* A) Gene expression data from the Allen Human Brain Atlas was summarised to the Desikan-
299 Killiany Atlas. B) We conducted PCA on the gene expression matrices (68 regions * 8235 genes) and two
300 components were justified with validity checks. C) We rotated these two components, and the component
301 scores show the relative positions of the 68 Desikan-Killany regions on these components. D) *g* ~ brain
302 cortical morphometry associations were calculated for three cohorts. E) The *g* ~ brain cortical
303 morphometry associations were meta-analysed with random effects models. F) The meta-analysed
304 standardised β values of each regional morphometry metric (cortical volume, surface area and thickness)
305 show their associations with *g*. G) Spatial associations were tested between the brain-regional component
306 scores for gene expression and the regional *g* ~ brain cortical morphometry associations. Then, controlling
307 for the regional component scores, *g*-associations for individual genes were calculated.

308 **Two major dimensions of cortical gene expression**

309 The Allen Human Brain Atlas consists of a high-resolution mapping of gene expression to
310 the cerebral cortex for *N* = 6 donors (5 male, 1 female, Age *M* = 42.50 years, *SD* = 13.38
311 years, range = 24-57 years). French and Paus (53) summarised these data across donors
312 to find the average gene expression values for each region in the Desikan-Killiany atlas,
313 and provide a method of quality control for between-donor consistency in regional gene
314 expression profiles, which results in retention of 8325 genes (out of 20,737 originally
315 available from the atlas). These retained genes are associated with neural gene ontology

316 (GO) terms, and those not retained tend to have low expression across the cortex or are
317 associated with other GO terms e.g. olfactory receptor and keratin genes (53). This results
318 in a gene expression matrix (rows = 68 cortical regions, columns = 8235 genes) of median
319 gene expression values for each region for each gene across donors. Initial results of a
320 principal component analysis (PCA) on these data indicated that regional variation in
321 gene expression across the cortex occurs across very few biological dimensions (see
322 *Figure 1B*); that is, there was much similarity across genes in the patterning of their
323 expression across brain regions. Mindful of the potential limitations of basing a new
324 discovery in fundamental neuroscience on a modest *post mortem* dataset (N = 6 donors),
325 we performed extensive checks.

326 We tested the factor congruence of the resulting principal components in terms of: over-
327 reliance on specific cortical regions, congruence with nine different gene expression data
328 processing pipelines, in two independent samples, and different brain parcellation
329 choices. First, to test the regional dependence of the principal components, we used
330 cross-validation to create 5 random partitions of the 68 regions 50 times without
331 replacement. Each time, the partitions were arranged into two sets, one with ~54-55
332 regions (4 of 5 partitions) and the other with ~13-14 regions (1 of 5 partitions). The PCA
333 was repeated for each iteration (a total of 250 tests). Absolute coefficients of factor
334 congruence between the two sets tended to be high for the first two components (PC1: M
335 = 0.926, SD = 0.064; PC2: M = 0.830, SD = 0.092), and were notably weaker, with higher
336 variability, from the third component onwards, see *Figure 2c*. Therefore, the first two
337 components do not rely heavily on individual regions, and so were taken forward in the
338 current analysis. Unrotated, PC1 accounted for 31.9% of the variance, and PC2 for 17.5%,
339 (after varimax rotation PC1 accounts for 25.8% of the variance, and PC2 for 23.6%).

340 Although there are efforts towards developing standardised processing of gene
341 expression data (54), there remains no general consensus. There have been several
342 proposed pipelines for summarising the Allen Human Brain Atlas data, and so we sought
343 to test whether the gene expression components derived using PCA are valid when the
344 data are summarised with different processing choices. We applied the scripts provided
345 by Markello et al. (54), that reproduce the pipelines for several studies (see *Table S6*). The
346 initial number of retained genes, and the number of genes matched to French and Paus'
347 post-consistency check genes are in *Table S8*. We investigated whether the two identified

348 components are similar when different methods of summarising the Allen Human Brain
349 Atlas to Desikan-Killiany space. To test this, we replicated the gene expression matrix
350 from French and Paus using Markello et al.'s scripts (54) and the abagen toolbox (55).
351 This replication is not exact, but very close – 8108 genes were retained and the factor
352 congruence coefficient for PC1 = 0.99, and for PC2 = 0.98. We then ran PCAs on the
353 resulting gene expression matrices obtained from nine gene expression data processing
354 pipelines54, see *Table S3*. For each pipeline, we calculated factor congruence coefficients
355 with French and Paus' method based on matched genes. Absolute coefficients ranged
356 from 0.93-0.97 for PC1 and 0.24-0.72 for PC2, see *Figure 2.* There are notable *PC2*
357 inconsistencies with particular pipelines - Burt (2018), Anderson (2020), Liu (2020) and
358 Markello (2021) - which are likely due to less common choices such as donor-specific
359 probe selection, stringent interareal similarity filtering thresholds, and other choices that
360 impact the number of genes retained.

361 We limited the donor age from these additional datasets to be in proximity to the age
362 range of the Allen Human Brain Atlas (24-57 years of age). See *Table S1* for descriptive
363 statistics of the validation samples. The test for between-donor consistency provided by
364 French and Paus (58) was applied to these datasets. Then, PCAs were conducted on the
365 gene expression matrices (rows = cortical regions, columns = genes), and genes were
366 matched with those in the Allen dataset to test for factor congruence. Summaries of the
367 number of retained genes at each step are in *Table S7*.

368 To test whether the first two components were generalizable beyond the 6 donors from
369 which the Allen Human Brain Atlas data were derived, we sought external validation with
370 two independent datasets, the BrainSpan Atlas https://www.brainspan.org/ and an atlas
371 provided by Kang et al. connected to the Human Brain Transcriptome Project
372 https://hbatlas.org/56. Both external datasets used the Affymetrix GeneChip Human Exon
373 1.0 ST Array Platform to summarise gene expression data. and include 11 cortical regions,
374 which have previously been roughly matched to 14 regions in the Desikan Killiany
375 atlas57 (see Figure S1). For BrainSpan (donor N = 5), these are collapsed across
376 hemispheres, but for the Kang et al. dataset (donor N = 11), they are available for each
377 hemisphere separately (a total of 22 regions). Genes with consistent between-donor
378 profiles were identified, using French and Paus' procedure58. To test for factor
379 congruence, these were then matched with the 8235 genes that were consistent between

donors in the French and Paus dataset, resulting in 2250 genes for the BrainSpan comparison and 908 for Kang et al.. The relatively small numbers of retained genes could be due to different cortical boundaries, extent of cortical coverage or the gene expression measurement and sampling methods used. There was high factor congruence for $PC1_{Allen}$ in both datasets (the coefficient for $PC1_{BrainSpan}$ = 0.88 and $PC1_{Kang\ et\ al.}$ = 0.96) and low-moderate factor congruency for $PC2_{Allen}$ (with $PC2_{BrainSpan}$ = 0.24, and $PC3_{Kang\ et\ al.}$ = 0.63 (see *Figure 2E*). $PC2_{Kang\ et\ al.}$ did not have high factor congruence with any Allen component (the maximum absolute value was 0.19, which was with $PC6_{Allen}$).

Lastly, we tested whether the positioning of regional boundaries affected the consistency of the components (see *Figure 2F*). Three open source atlases were tested: Yeo's Functional Connectivity *7* and 17 Network atlases (with 7 and 17 regions, respectively)59 and the Destrieux atlas (134 regions, 67 per hemisphere)60. For all three, as with the Desikan-Killiany atlas, 8108 genes matched with the 8235 from the main working dataset. Again, factor congruence coefficients tended to be higher for $PC1_{Allen}$ than $PC2_{Allen}$, ($PC1_{Yeo7}$ = 0.85, $PC1_{Yeo17}$ = 0.96, $PC1_{Destrieux}$ = 0.81; $PC2_{Yeo7}$ = 0.12, $PC2_{Yeo17}$ = 0.35, $PC2_{Destrieux}$ = 0.65). Notably, factor congruence coefficients tended to increase for PC2 with increasing granularity. These results may partially explain why $PC2_{BrainSpan}$ was less with $PC2_{Allen}$ (11 regions, less granular) compared to $PC2_{Kang\ et\ al.}$ (22 regions, more granular).

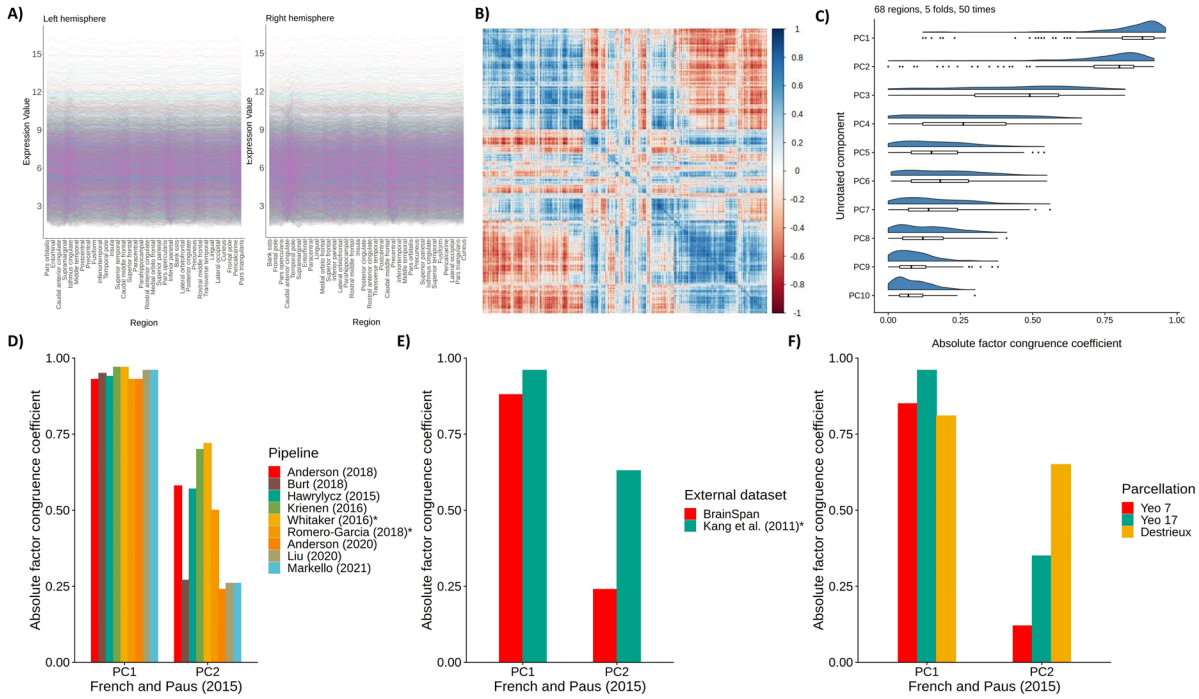

Figure 2 Validating gene expression components.

Figure 2 note A) Raw gene expression values for the 34 regions for the left and right hemispheres, for the 8235 consistent genes. B) Correlation plot of the 8235 genes across the 68 cortical regions (8235 * 8235). C) Absolute factor congruence coefficients for the first 10 components between "train" and "test" folds (~54-55 regions, and ~12-13 regions), over 50 repetitions. D) Absolute factor congruence coefficients from different pipelines with PC1 and PC2 of the current dataset of interest, using the Desikan-Killiany atlas. * denotes that PC3 from that pipeline is compared with PC2. E) Absolute factor congruence coefficients for two external datasets with PC1 and PC2 of the current dataset of interest. * denotes that PC3 from is compared with PC2. F) Absolute factor congruence coefficients for three alternative parcellations with the PC1 and PC2 of the current dataset (which uses the Desikan-Killiany atlas).

In summary, just two components explain the majority of gene expression variation across the human cerebral cortex. Unrotated, PC1 accounted for 31.9% of the variance, and PC2 for 17.5%, (after varimax rotation PC1 accounts for 25.8% of the variance, and PC2 for 23.6%). They are not heavily reliant on individual regions, nor are they donor-specific. The first component is robust across all validation tests but, for the second, we note some effects of cortical boundary positioning, sampling differences, and the number of retained genes – factors which can partly be attributed to technical confounds. With these results in mind, we extracted two components, which together account for 49.4% of the variance, with varimax rotation for further analysis.

418 **Interpretation of gene expression components**

419 To aid interpretation of the two components, we conducted statistical
420 overrepresentation analyses, at http://geneontology.org/, which is powered by
421 PANTHER (61). The results suggest that Component 1 represents cell-signalling and post-
422 translational modification processes (with loadings < -0.3 providing upregulation and
423 those > 0.3 providing downregulation) (see *Figure 3* and the supplementary data file for
424 full GO results and component loadings). Prominent GO terms include i) amino acids and
425 organic compounds, which provide energy to cells and hasten chemical reactions
426 necessary for post-translational modifications, and ii) signalling terms, which convey
427 information about nutrients in the environment and support coordination between cells.
428 Component 2 is a transcription factors axis (with loadings < -0.3 providing
429 downregulation and those > 0.3 providing upregulation). The GO terms implicate
430 biosynthesis, binding and RNA polymerase II, defining characteristics of transcription
431 factors.

432 Additionally, we tested whether the distribution of component loadings differed by cell-
433 type. Zeisel et al. (62) identified proteins expressed in 9 specific cell-types, from single-
434 cell transcriptomes of 3005 cells in the mouse somatosensory cortex and hippocampus.
435 Shin et al. (63) converted these genes to human gene symbols, with the HologoGene
436 database (64). We matched these genes with those available in our current dataset (N =
437 8235 genes). Out of the initial set of cell-specific genes, in our dataset there were 129/214
438 astrocytes, 204/357 CA1 pyramidal neurons, 127/321 endothelial cells, 191/415
439 ependymal cells, 181/293 interneurons, 185/374 microglia, 60/133 mural cells,
440 139/393 oligodendrocytes, 155/236 S1 pyramidal neurons, and the remaining 6864
441 proteins were "unclassified", and treated as a baseline group.

442 Descriptive statistics of component loadings for each cell-type are in *Table S3* and the
443 results of the Dunn posthoc tests are in *Tables S4 and S5.* Generally, the loadings of
444 different cell types tend to be skewed. For Component 1, loadings for all but ependymal
445 and interneuron cell types have an absolute skewness value > 0.228. For Component 2,
446 all but endothelial cells have absolute skewness > 0.187. This skewness in loadings
447 suggests that specific cell types play a particular roles in the regulation of the two
448 components. We investigated whether specific cell types load on the two major

449 components in ways that deviate from the average distribution of unclassified loadings.
450 Loading distributions by cell type are shown in *Figure 3* (bottom panel) and descriptive
451 statistics and full results of Dunn posfthoc tests, with *p*-values adjusted with the Holm
452 method, are in *Tables S3-5*. There are main effects of cell classification for both
453 components (Component 1: $H(9) = 88.986$, $p = 2.6e-15$, Component 2: $H(9) = 81.046$, $p =$
454 $1.001e-13$).

455 For Component 1, the unclassified set's distribution tends towards the expression side of
456 the axis ($M = 0.14$, $SD = 0.49$, skewness = -0.145). This contrasts with astrocytes ($z = -4.05$,
457 $p = .002$; $M = -0.04$, $SD = 0.49$, skewness = 0.375), CA1 pyramidal neurons ($z = 05.12$, $p =$
458 $1.36-05$; $M = -0.03$, $SD = 0.50$, skewness = 0.254) and microglia ($z = -5.60$, $p = 1.86e-09$; M
459 $= -0.11$, $SD = 0.46$, skewness = 0.506), which are skewed towards the regulation side. For
460 the second component, the unclassified set of genes tend towards regulating
461 transcription factors ($M = 0.15$, $SD = 0.46$, skewness = -0.183). Whereas, S1 pyramidal
462 cells oppose this direction ($z = -5.03$, $p = 1.98e-08$; $M = -0.05$, $SD = 0.47$, skewness = 0.200),
463 astrocytes and microglia fall more sharply on the regulation side than the unclassified set
464 of genes (unclassified kurtosis: 1.925; astrocytes: $z = 3.89$, $p = .003$, kurtosis = 2.582;
465 microglia: $z = 5.41$, $p = 2.66e-06$, kurtosis = 2.846). For all other comparisons between the
466 unclassified cells and individual cell types, $p = 1$.

467 Additionally, through FUMA https://fuma.ctglab.nl/ we tested whether the genes with
468 absolute loadings > 0.3 on each component were significantly related to gene sets in the
469 GWAS catalog. There were no significant ($\alpha = .05$) associations for either component,
470 demonstrating the highly general nature of the two components of cortical gene
471 expression.

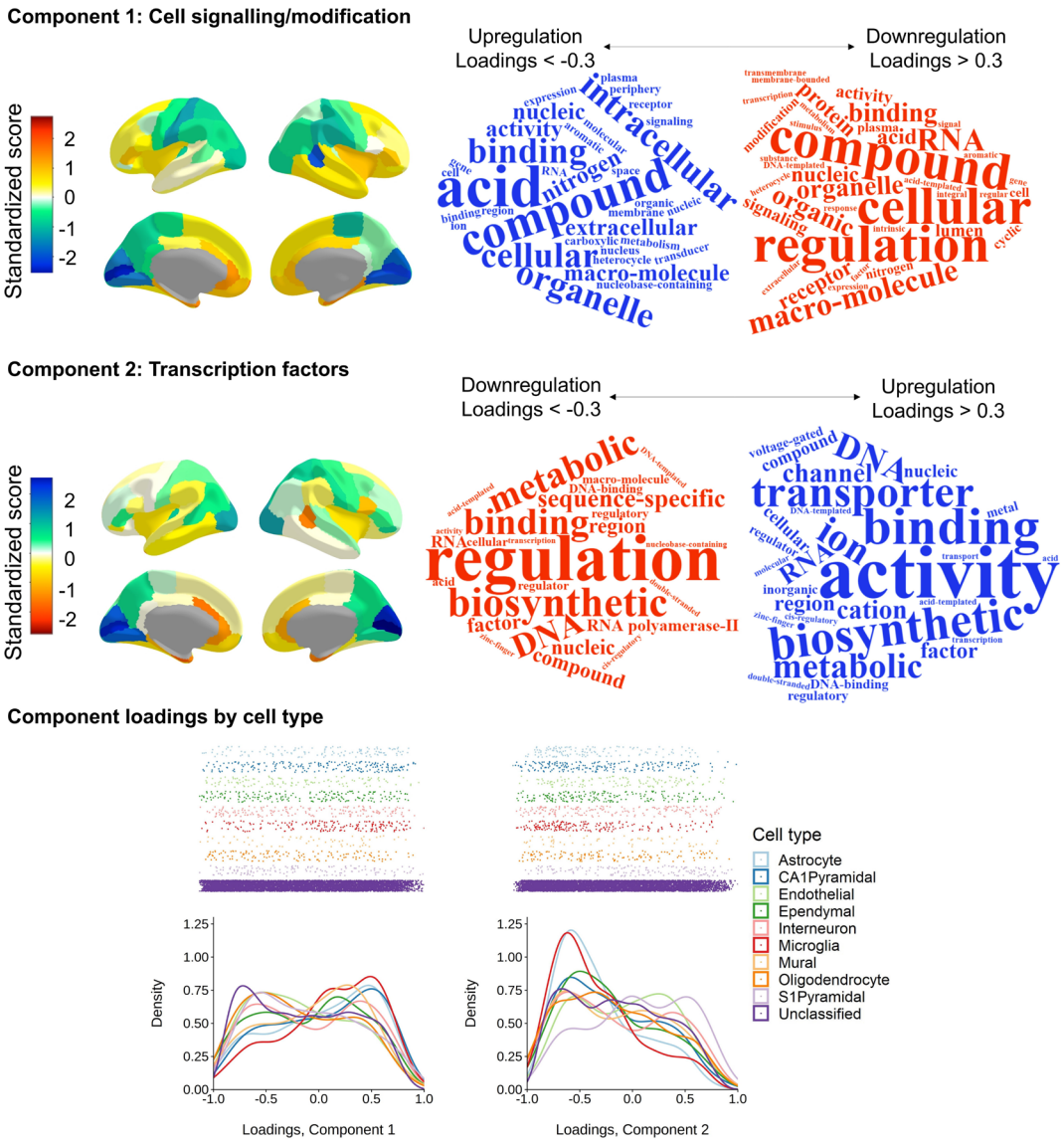

Figure 3 Two major components of cortical gene expression.

Figure 3 note Top and middle panels (Component 1 and Component 2, respectively) left: Regional *z* scores mapped to the cerebral cortex (scaled for each hemisphere) and right: word clouds of the statistical over-representation results. The relative direction of component scores is arbitrary (dictated by the PCA), and here, the colour scale is flipped between components so that the directions of upregulation/downregulation match. Bottom panel: Density distribution plots of loadings on Component 1 and Component 2 coloured by cell type.

Regional distribution of component scores across the cerebral cortex

The component scores were scaled to correct for interhemispheric differences in gene expression values (see Methods for details). These component scores were then mapped to the 68 Desikan Killany regions (see *Figure 4* and *Table* S9). There was a strong interhemispheric correlation in scores between the 34 paired regions for both

485 Component 1 (r = 0.815, p = 4.411e-09) and Component 2 (r = 0.725, p = 1.25e-06).
486 Parietal and occipital regions are on the upregulation side of Component 1 (cell
487 signalling/modification), with frontal and temporal regions indicating downregulation.
488 For Component 2 (transcription factors), lateral frontal areas tend towards balance
489 between upregulation and downregulation, whereas medial frontal regions tend towards
490 downregulation and parietal and occipital regions towards upregulation. For both
491 components and in both hemispheres, the highest absolute scores are observed in the
492 medial occipital regions (pericalcarine, cuneus and lingual), which fall strongly on the
493 upregulation side of both components.

494 We tested whether the regional mean morphometry profiles (*see Supplementary Text 1*)
495 are associated with regional gene expression component score patterning. In general, the
496 thicker a region is, the more strongly it falls on the downregulation side of both gene
497 expression components (Component 1: r = 0.764, p = 3.67e-14 and Component 2: r = -
498 0.799, p = 3.132e-16). Associations between mean regional surface area patterns and
499 both components were small-to-moderate (Component 1: r = -0.230, p = .059, Component
500 2: r = 0.245, p = .044), and between mean regional volume and both components were
501 small and not statistically significant at the $\alpha < .05$ level (Component 1: r = -0.082, p =
502 .504, Component 2: r = 0.111, p = .368).

503 **Cortical morphometric associations with general cognitive ability *(g)* – Meta-**
504 **analyses (*N* = 40,929)**

505 We first used raw data from three cohorts to estimate regional associations between
506 three MRI-derived morphometry measures (cortical volume, surface area and thickness)
507 and *g* (total *N* = 40,929; three cohorts – the UK Biobank (UKB, 65,
508 http://www.ukbiobank.ac.uk): *N* = 39,250 participants (53% female), age *M* = 63.91
509 years (*SD* = 7.67 years), range = 44-83 years; STRADL (66, a Generation Scotland imaging
510 sample): *N* = 1043 participants (60% female), age *M* = 59.29 years (*SD* = 10.12 years),
511 range = 26-84 years; and the Lothian Birth Cohort 1936 (LBC1936, 67,68
512 https://www.ed.ac.uk/lothian-birth-cohorts): *N* = 636 participants, (47% female), age *M*
513 = 72.67 years, *SD* = 0.41 years, range = 70–74 years). General cognitive function (*g*) scores
514 were derived using confirmatory factor analysis (in a structural equation modelling
515 framework) in each of the three cohorts using multi-domain cognitive test batteries, and

each individual test score was corrected for age and sex. As one of the most replicated phenomena in psychological science, *g* is based upon the tendency for performance on all cognitive tests to be correlated, and is generally invariant to cognitive test content, provided that multiple domains are captured (69). These properties lend it well to cross-cohort genetic analyses (23), for example, and we leverage them here.

Latent *g* scores were extracted for all participants, and associations with three measures of cortical morphometry (volume, surface area and thickness) were estimated for each of the 68 regions in each cohort. Cortical measures were controlled by age, sex, head position in the scanner (X, Y and Z coordinates), testing site (for UKB and STRADL) and lag between cognitive and MRI testing appointments (for LBC1936). For UKB, X, Y and Z co-ordinates were calculated relative to one target participant, and for LBC1936 and STRADL, they were taken from the mri_info -cras flag output. Standardised β estimates of the association in each brain region between *g* and each brain morphometric property (volume, surface area, thickness); these were computed for each cohort. There were strong cross-cohort correlations between the 68 regions for all *g*-associations (see *Table 1*).

Table 1 Cross-cohort correlations of regional *g*-associations.

Table 1 note (all $p < .001$).

Cohort comparison	*g* ~ volume	*g* ~ surface area	*g* ~ thickness
LBC1936–STRADL	$r = 0.52$	$r = 0.40$	$r = 0.59$
STRADL–UKB	$r = 0.67$	$r = 0.69$	$r = 0.70$
UKB–LBC1936	$r = 0.64$	$r = 0.55$	$r = 0.68$

We then ran a random effects meta-analysis on the standardized β values. The meta-analytic results of the three cohorts' associations between *g* and brain morphometry data (68 regions x 3 measures = 204 meta-analyses) are summarised in *Figure 4* and reported in detail in *Tables S19-S21*. Meta-analysed standardised βs for *g*-volume associations *M* β = 0.100 (SD = 0.035, range from 0.017 to 0.172), for *g*-surface area, *M* β = 0.098 (SD = 0.028, range from 0.018 to 0.148), and for *g*-thickness associations *M* β = 0.032 (SD = 0.035, range = -0.047 to 0.123).

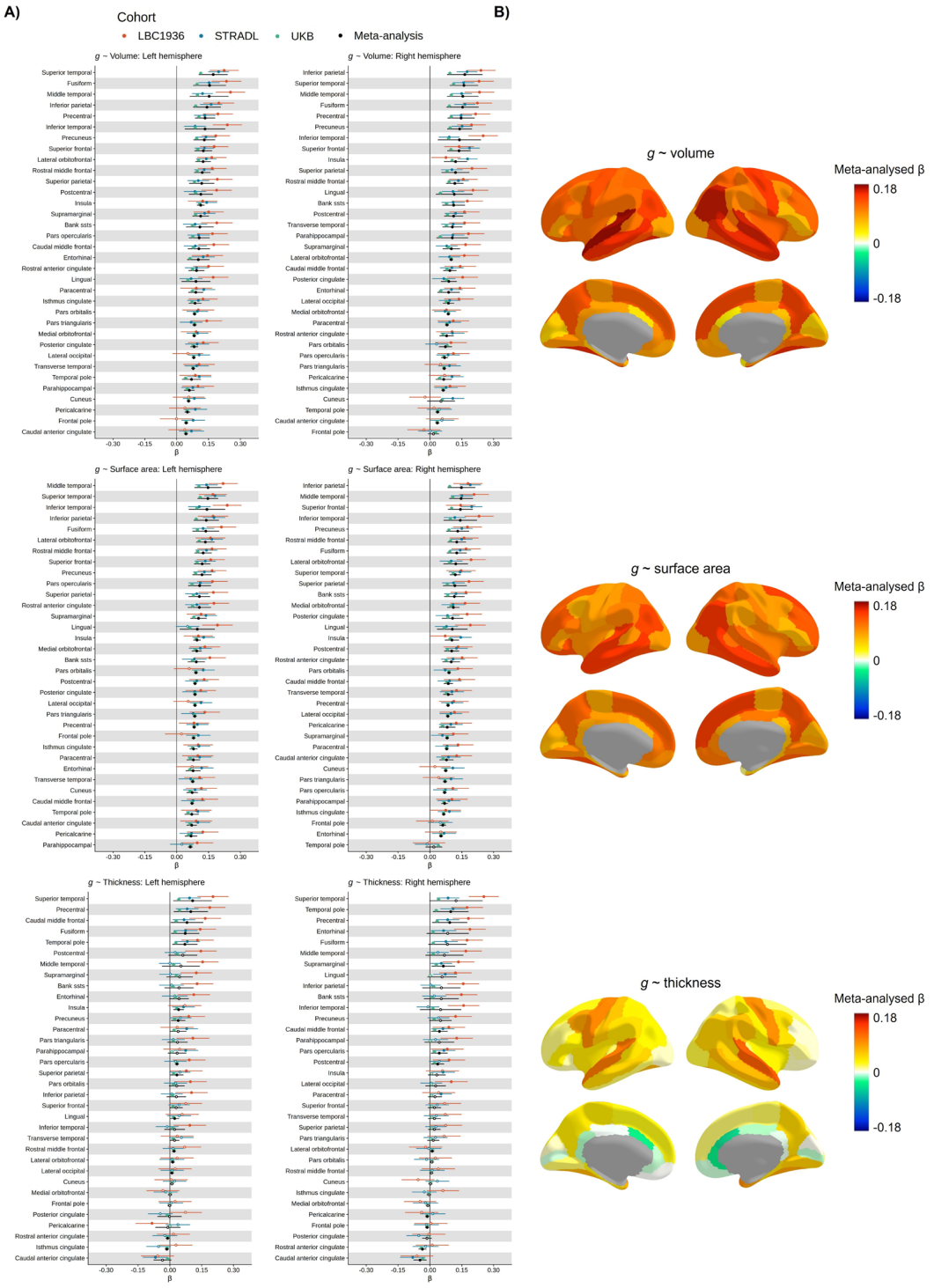

Figure 4 Meta-analysed brain regional associations with *g*.

Figure 4 note A) Standardised β estimates mapped to the cerebral cortex. B) Meta-analysed standardised β estimates for *g*-volume, *g*-surface area and *g*-thickness. Those for which $p < .05$ are filled in, and those for which $p > .05$ are outlined. The y-axis is ordered by the meta-analysed β values.

The current results provide support for theories (25,26) regarding which regions are key in brain morphometry-*g* associations. Parietal and frontal regions generally have relatively strong *g*-associations with volume and surface area, though not with cortical thickness. For volume and surface area, all temporal regions had relatively high *g*-associations mean β = 0.152 and 0.141, for volume and surface area respectively, and the superior temporal region had the strongest *g*-volume association (left β = 0.172) and *g*-thickness association (right β = 0.123) of all regions. Some of the highest *g*-volume and *g*-surface area associations are for the fusiform and inferior parietal regions (*g*-volume β range = 0.143 to 0.164; and *g*-surface area β range = 0.137 to 0.143). The precuneus regions also have among the overall highest associations (mean precuneus *g*-volume β = 0.135, and *g*-surface area β = 0.125), in line with updated reports of regional *g*-associations (70, 26).

There is high inter-hemispheric consistency for each of the meta-analytic *g*-morphometry associations: volume (r = 0.880, p = 6.836e-12), surface area (r = 0.810, p = 6.97e-09), and thickness (r = 0.881, p = 6.04e-12), see *Figure S11*. In addition, estimates were strongly correlated between *g*-volume and *g*-surface area associations (r = 0.812, p < 2.2e-16), and moderately correlated between *g*-volume and *g*-thickness (r = 0.594, p = 9.351e-08). As anticipated, based on previous work showing phenotypic and genetic distinctions between surface area and thickness (28,29,30,31), the correlation between *g*-surface area and *g*-thickness estimates was small and not statistically significant at the α < .05 level (r = 0.135, p = .271).

To help interpret why some regions might have higher associations with *g* than others, we tested correlations between regional *g*-associations and the regional mean profiles of volume, surface area and thickness (reported in *Supplementary Text 1*). The regional *g*-associations were positively associated with the corresponding regional mean profiles for all three morphometry measures. Volume had the strongest correlation (r = 0.714, p = 8.444e-12), followed by surface area (r = 0.602, p = 5.523e-08), and then thickness (r = 0.328, p = .006). In other words, regions with stronger *g*-associations tend to be larger in terms of volume and surface area, and also moderately tend to be thicker.

We then tested whether larger and thicker brain regions are more strongly associated with *g* because they tend to be better proxies for whole-brain measures (as they

577 contribute more to the total measure). The maginitude of total brain *g*-volume and *g*-
578 surface area associations are in line with the maximum of the individual regions – *g*-
579 whole cortex volume (β = 0.179, SE = 0.035, p < .0001), *g*-whole cortex surface area (β =
580 0.154, SE = 0.021, p < .0001). As there are some negative *g*-thickness associations, the *g*-
581 whole cortex thickness associaiton was weaker than the regional maximum (β = 0.073,
582 SE = 0.037, p = 0.049). We then corrected regional *g*-associations for these total brain
583 measures, and correlated regional profiles with and without correction. These
584 correlations are moderate-to-strong: *g*-volume (r = 0.606, p = 4.26e-08), *g*-surface area
585 (r = 0.590, p = 1.19e-07), and *g*-thickness (r = 0.933, p < 2.2e-16), suggesting that it is not
586 only because larger/thicker brain regions are a better proxy for the whole brain measure
587 that they are more strongly associated with *g*.

588 **Interregional variation in gene expression corresponds to interregional variation**
589 **in cognitive function**

590 Next, we tested whether brain regions' differences in gene expression (as measured using
591 the two components we described earlier) are correlated with *g*-morphometry
592 associations. That is, we asked whether brain regions for which morphometric measures
593 (volume, surface area and thickness) are more strongly related to *g* were also more
594 strongly related to general dimensions of gene expression.

595 We tested linear correlations between the absolute component scores of gene expression
596 and the meta-analysed standardised β scores for cortical morphometry associations with
597 *g*, and also report the comparable quadratic regression results with non-absolute scores
598 (see *Table 2* and *Figure 5*). There were negative associations for all analyses, and those
599 for *g*-volume and *g*-surface area were moderate-to-strong and statistically significant at
600 the α < .05 level. These results suggest that, generally, regions more strongly associated
601 with *g* tend to be more balanced between the downregulation and upregulation sides of
602 both cell-signalling/modification and transcription factors components.

603 There were no correlations between regional mean expression (for the mean regional
604 values M = 6.06 (SD = 0.046), range = 5.98 to 6.18) and *g*-brain morphometry association
605 profiles for which p < .05 (*g*-volume r = -0.038, p = .761; *g*-surface area r = -0.051, p = .682;
606 *g*-thickness r = 0.062, p = .616), demonstrating the value of the PCA approach as

associations between genome-wide dimensions of expression and *g* are not reducible to an average brain-wide pattern of gene expression.

Table 2 Correlations of correlations: Meta-analysed *g*-cortex associations with two major gene expression components.

Table 2 note. Pearson's *r* values for the correlation between brain-g associations and brain-gene expression component profiles. Note that these are for linear associations using the absolute gene-expression component scores. Results for the equivalent associations using the non-absolute components scores (quadratic component) are presented in *Table S25* and *Figure 5*, which illustrates the balance between downregulation and upregulation.

g ~	Component 1	Component 2
Volume	*r* = -0.383, *p* = .001	*r* = -0.578, *p* = 2.5e-07
Surface area	*r* = -0.325, *p* = .007	*r* = -0.470, *p* = 5.3e-05
Thickness	*r* = -0.168, *p* = .172	*r* = -0.277, *p* = .002

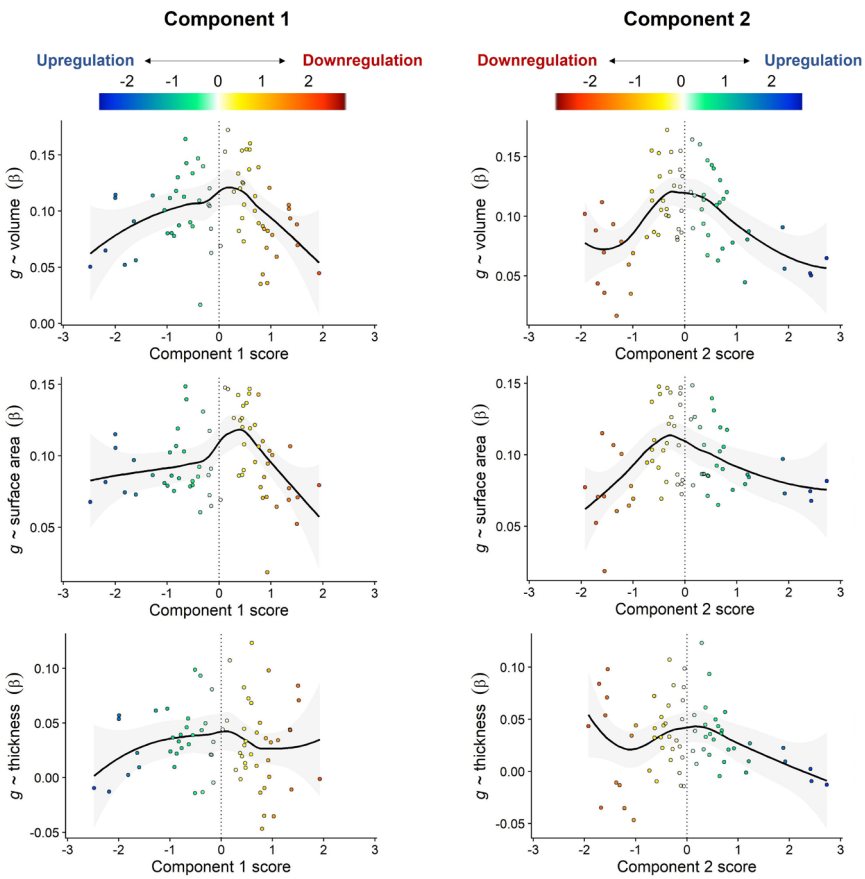

Figure 5 Associations between regional-*g* profiles and the two gene expression components.

Figure 5 note LOESS functions are plotted (the quadratic model results are comparable to the absolute score correlations, and are presented in *Table S25*). A vertical line at component scores of 0 represents a balance between upregulation and downregulation ends of each component. The colour scale is flipped between Components, so that the direction of downregulation and upregulation match.

Associations between *g* and individual genes

Lastly, we tested for individual *g*-gene expression pattern associations, controlling for the two general components of gene expression . All mean expression scores were calculated per region, and then scaled separately for left and right hemisphere regions, to account for sample-based artifacts in hemisphere differences in expression values, in line with the method for the component scores. After FDR correction (threshold = $Q < .05$), there were 517 individual genes whose cortical patterning was correlated with *g*-volume patterning, 487 with *g*-surface area and 531 with *g*-thickness (these results are available in detail in the supplementary data file). 217 were shared between *g*-volume and *g*-surface area, 182 between *g*-volume and *g*-thickness and 35 between *g*-surface area and *g*-thickness. 34 genes with *FDR Q* < .05 overlapped for all three morphometry measures (|β| range = 0.14 to 0.55, see *Figure 6*). These genes are particularly likely candidate substrates of *g.* Some regional expression profiles have positive associations with *g*-cortical measure profiles, while others have negative associations. For discussion, genes with negative *g*-associations in the present study are marked with an asterisk.

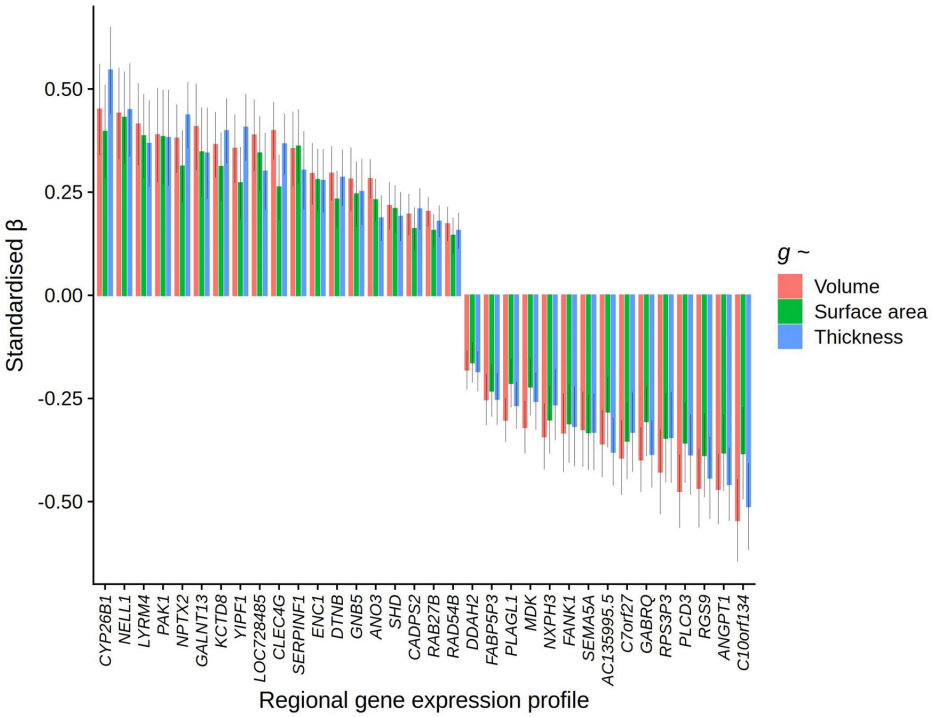

Figure 6 Specific associations between regional g-morphometry profiles and individual gene expression profiles.

Figure 6 Note Standardised β for specific individual gene profiles (i.e. corrected for general components of gene expression) for which FDR Q > .05 for all three cortical morphometry associations with g.

642 Several of these 34 genes have been previously reported to be associated with
643 Alzheimer's Disease: overexpression of *ANGPT1** has been found to increase amyloid beta
644 secretion (71) whilst *CLEC4G* suppresses amyloid beta (72), and increased levels of *ENC1*
645 (73,74) and *NPTX2* (75,76,77,78) are consistently demonstrated to have protective
646 effects against cognitive decline in Alzheimer's disease. Other genes from this list have
647 been associated with other neurodegenerative disorders – for example. Loss of *GABRQ**-
648 containing neurons is an indicator of early social-emotional cognitive decline in
649 frontotemporal dementia (79), *RAB27B* regulates α-Synuclein, which is a primary
650 indicator of Parkinson's disease and dementia with Lewy bodies (80), and *DTNB* is an
651 indicator of extent of neuronal injury and inflammation in Alzheimer's disease (81).
652 Additionally, *SEMA5A** has previously been associated with hippocampal volume and
653 performance on cognitive tests (82). *GNB5* plays a key role in several
654 neurodevelopmental cognitive disabilities (83,84). *CYP26B1* is upregulated in the
655 prefrontal cortex (85), and there are links between its catabolism in the hippocampus
656 and poor cognitive outcomes in mice (86).

657 Other individual genes associated with *g*-cortical profiles have been associated with
658 cognitive functioning more generally, for example, *RGS9** has been implicated in motor
659 coordination and working memory (87), *CADPS2* is associated with cognitive ability and
660 memory in healthy adults (88), and *FANK1** has been found to have genome-wide
661 significant associations with *g* in CHARGE-COGENT and UKB cohorts (23). Some others
662 have been linked to cognitive disorders, for example *LYRM4* with schizophrenia (89), and
663 *DDAH2** with multiple neurological conditions and psychiatric disorders (90). Previous
664 GWAS associations with these 34 genes were identified in FUMA and are available in the
665 supplementary data file. Recurrent associations include educational attainment, body
666 mass index (BMI), brain measurements, coronary artery disease, schizophrenia, and
667 depression (see the supplementary data file). *C10orf134*, NELL1*, *RAD54B* and *GALNT13*
668 have previous GWAS associations with educational attainment, and *MDK** has previous
669 GWAS associations with schizophrenia. Potential novel, or less-studied, individual gene
670 substrates of complex cognitive processing identified in the present study include:
671 *AC135995.5*, ANO3*, *C7orf27**, *FABP5P3**, *KCTD8*, *LOC728485*, *NXPH3**, *PAK1*, *PLAGL1**,
672 *PLCD3*, RPS3P3*, SERPINF1*, *SHD* and *YIPF1*.

Discussion

This study reveals and validates a fundamental organisation principle of cortical gene expression patterns across the human brain. We then use this information to identify the shared and specific aspects of regional cortical gene expression and show that they are associated with regional brain-structure correlates of complex thinking skills. We also show that this information is not obtainable by simply considering aggregate/mean levels of gene expression across regions.

We validated our discovery of two major components of interregional variation in gene expression: one indicating cell-signalling/modifications and the other, transcription factors. Using the largest meta-analysis of the cortical loci of general cognitive functioning (*g*) to-date, we find that regions that are more balanced between downregulation and upregulation of these two gene expression components are most strongly associated with *g.* Controlling for these established patterns of gene expression covariation allowed us to identify which individual genes had spatial expression patterns that specifically reflect cortical correlates of *g*, beyond the major dimensions of gene expression. Critically, without this approach, one is likely to miss or erroneously ascribe an interpretation to an individual gene, as its profile is confounded by major components of shared spatial covariation across multiple gene expression patterns.

We conducted one of the largest analyses of *g*-cortical morphometry associations to-date. These associations are generally in line with the parieto-frontal integration theory (P-FIT, 25) and strengthens support for the involvement of regions (e.g., temporal, precuneus) that were not included in earlier iterations of the model. There was strong agreement across the three cohorts in the magnitudes and spatial patterning of associations, which speaks to the validity of *g* as a measure of cognitive ability (indicated by different cognitive tests included by each cohort). The consistency of results also indicates that careful harmonisation of image processing alongside careful attention to phenotype measurement may partially offset the apparent need for many thousands of participants to obtain replicable brain-behaviour association results (27).

Turning to the gene expression components-*g* correlations, the more strongly regions were associated with *g*, the more they tended towards the balance between the downregulation and upregulation sides of the cell-signalling/modification and

transcription factors components. Complex cognitive functions therefore appear to be facilitated at a happy medium on each of these components. Other regions that fall on either the downregulation or upregulation sides of each of the two major dimensions perhaps specialise in less general functions. An important question this raises, but we cannot answer here, is whether individual differences in the balance of gene expression in these cortical dimensions might partly explain why people differ from each other in their general cognitive functioning.

Using this newly-gleaned information about what is common among gene expression profiles, we then identified 34 individual genes whose spatial expression was correlated with *g* cortical patterning, independent of the two major dimensions. Whereas some of the genes strongly indicated in the two major dimensions themselves could also pertain, causally, to mechanisms and processes underpinning *g,* the nature of shared expression patterns as presented here disallows that direct inference for individual genes. In contrast, these 34 genes with specific associations are particularly strong candidates for playing a role in facilitating complex cognitive processes. Several of these genes have been previously identified as associated with various cognitive outcomes, whilst others are potentially novel substrates of cognition.

This study has several strengths and limitations. As we quantitatively demonstrate, the present approach surpasses candidate gene and median expression information, clarifying our understanding of the molecular substrates of complex cognitive abilities in the human brain. We extensively validate the discovered components of gene expression, mitigating concerns that this finding might be an artefact of a small number of donors in a single sample. The first component is highly consistent across different datasets, gene expression data processing and summary choices, and brain regional parcellation choices. Although the second component does not depend heavily on individual regions, it is somewhat affected by the granularity and boundaries of the parcellation, gene expression data sampling and processing choices, and the number of genes retained. While efforts continue to standardize gene expression processing pipelines (91), the effects of different choices on dimensions of between-gene covariances should continue to be considered. As donor contributions to gene expression databases continue to increase, brain regional summaries of gene expression will become more precise. Several genes were excluded from the current analysis due to low between-donor consistency.

Although this is partially due to some of these genes having generally low expression across the cortex, there also appears to be an effect of the sampling methods of gene expression data. Gene expression sampling methods consistent with clear cortical boundaries and full cortical coverage will increase between-donor consistency in regional gene expression profiles and enable stronger tests of external validity.

We leveraged the fact that the UKB, STRADL and LBC1936 cohorts have adopted comparable methods, including similar MRI processing pipelines with FreeSurfer http://surfer.nmr.mgh.harvard.edu/, and collection of various cognitive test scores, which enabled us to harmonise the processing and approach to the calculation of *g.* Consistency in the applied methods between cohorts allows for direct quantitative comparison. Despite these advantages, there were also some differences between MRI data and processing the three cohorts, which might differentially affect the cortical surface results: 1) each of the three cohorts used different scanners for MRI acquisition and, although T1-weighted data provides consistent between-scanner measures (92), we cannot rule out scanner-specific differences, 2) Desikan-Killiany parcellations were visually inspected and manually edited for LBC1936 and STRADL, but not for UKB (outliers $SD > 4$ were excluded), and 3) different FreeSurfer versions were used for each cohort, which is likely to have contributed to some differences in estimations, alongside different types and quantity of cognitive tests. However, high between-cohort correlations suggest that these differences may not meaningfully affect the current results and provide evidence in support the use of *g* in meta-analytic studies to reach reproducible brain-cognition associations (93).

A separate limitation of this study is that all included participants were in relatively good health, as we chose to exclude participants with any declared neurodegenerative diseases. It is therefore not clear that the reported regional *g*-associations would generalise to clinical populations. Additionally, whereas the cognitive-MRI data do not include childhood and adolescence (and therefore the results may not relate directly to those parts of the life span), the good adulthood age coverage, absence of age moderation of the meta-analytic estimates within-cohort, and clear agreement across cohorts suggests that the exceptionally well-powered results reliably capture adulthood brain-*g* correlations.

In summary, this newly-possible study uses robust methods to advance our understanding of how gene expression is associated with complex cognitive functioning. We discovered and interpreted two general components of cortical gene expression, and identified general and specific patterns of gene expression that are candidate substrates that may contribute to some of the association between brain structure and complex cognitive functioning.

References

1 Parker, N. et al. Corticosteroids and Regional Variations in Thickness of the Human Cerebral Cortex across the Lifespan. *Cerebral cortex*, *30*, 575–586. 10.1093/cercor/bhz108 (2020).

2 Shin, J. et al. Cell-Specific Gene-Expression Profiles and Cortical Thickness in the Human Brain. *Cerebral cortex*, *28*(9), 3267–3277. 10.1093/cercor/bhx197 (2018).

3 Vidal-Pineiro, D. et al. Cellular correlates of cortical thinning throughout the lifespan. *Scientific reports*, *10*(1), 21803. 10.1038/s41598-020-78471-3 (2020).

4 Darby, M. M., Yolken, R. H., & Sabunciyan, S. Consistently altered expression of gene sets in postmortem brains of individuals with major psychiatric disorders. *Translational psychiatry*, *6*(9), e890. 10.1038/tp.2016.173 (2016).

5 Writing Committee for the Attention-Deficit/Hyperactivity Disorder, Autism Spectrum Disorder, Bipolar Disorder, Major Depressive Disorder, Obsessive-Compulsive Disorder, and Schizophrenia ENIGMA Working Groups et al. Virtual Histology of Cortical Thickness and Shared Neurobiology in 6 Psychiatric Disorders. *JAMA psychiatry*, *78*(1), 47–63. 10.1001/jamapsychiatry.2020.2694 (2021).

6 Lukk, M., Kapushesky, M., Nikkilä, J. et al. A global map of human gene expression. Nat Biotechnol 28, 322–324 (2010). https://doi.org/10.1038/nbt0410-322

7 Lenz, M., Müller, FJ., Zenke, M. et al. Principal components analysis and the reported low intrinsic dimensionality of gene expression microarray data. Sci Rep 6, 25696 (2016). https://doi.org/10.1038/srep25696

8 Bhaduri, A., Sandoval-Espinosa, C., Otero-Garcia, M. et al. An atlas of cortical arealization identifies dynamic molecular signatures. Nature 598, 200–204 (2021). https://doi.org/10.1038/s41586-021-03910-8

9 Burt, J.B., Demirtaş, M., Eckner, W.J. et al. Hierarchy of transcriptomic specialization across human cortex captured by structural neuroimaging topography. Nat Neurosci 21, 1251–1259 (2018). https://doi.org/10.1038/s41593-018-0195-0

10 Hansen, J.Y., Markello, R.D., Vogel, J.W. et al. Mapping gene transcription and neurocognition across human neocortex. Nat Hum Behav 5, 1240–1250 (2021). https://doi.org/10.1038/s41562-021-01082-z

11 Wagstyl et al. Transcriptional Cartography Integrates Multiscale Biology of the Human Cortex. bioRxiv 2022.06.13.495984; doi: https://doi.org/10.1101/2022.06.13.495984

12 Deary I. J. Intelligence. Annual review of psychology, 63, 453–482. 10.1146/annurev-psych-120710-100353 (2012).

13 Panizzon, M. S. et al. Genetic and Environmental Influences of General Cognitive Ability: Is *g* a valid latent construct?. *Intelligence*, *43*, 65–76. 10.1016/j.intell.2014.01.008 (2014).

14 Bijwaard, G. & Kippersluis, H. & Veenman, J. Education and Health: The Role of Cognitive Ability. Journal of Health Economics. 42. 29-43. 10.1016/j.jhealeco.2015.03.003. (2015).

15 Strenze T. Intelligence and socioeconomic success: A meta-analytic review of longitudinal research. *Intelligence*, 35, 401–426. 10.1016/j.intell.2006.09.004 (2007).

16 Wraw, C., Deary, I. J., Gale, C. R. & Der, G. Intelligence in youth and health at age 50. *Intelligence* **53**, 23–32, 10.1016/j.intell.2015.08.001 (2015).

17 Batty G. D., Deary I. J., Gottfredson L. S. Premorbid (early life) IQ and later mortality risk: Systematic review. *Annals of Epidemiology*, 17, 278–288. 10.1016/j.annepidem.2006.07.010 (2007).

18 Calvin, C. M. *et al*. Intelligence in youth and all-cause-mortality: systematic review with meta-analysis. *International Journal of Epidemiology* **40**, 626–644, 10.1093/ije/dyq190 (2011).

19 Dubois J, Galdi P, Paul LK, & Adolphs R. A distributed brain network predicts general intelligence from resting-state human neuroimaging data. *Philos Trans R Soc Lond B Biol Sci.* 373 (1756). 10.1098/rstb.2017.0284 (2018).

20 Zimmermann J, Griffiths J. D., McIntosh AR. Unique Mapping of Structural and Functional Connectivity on Cognition. *Journal of Neuroscience*. 38(45):9658–9667. 10.1523/JNEUROSCI.0900-18.2018 (2018).

21 Barbey A. K. et al. An integrative architecture for general intelligence and executive function revealed by lesion mapping. *Brain*. 10.1093/brain/aws021.135:1154–64. (2012).

22 Dawe, R. J. et al. Postmortem brain MRI is related to cognitive decline, independent of cerebral vessel disease in older adults. *Neurobiology of aging*, *69*, 177–184. 10.1016/j.neurobiolaging.2018.05.020 (2018).

23 Davies, G., et al. Study of 300,486 individuals identifies 148 independent genetic loci influencing general cognitive function. *Nat Commun* **9,** 2098 10.1038/s41467-018-04362-x (2018).

24 Camilleri, J. A., et al. Definition and characterization of an extended multiple-demand network. *NeuroImage*, *165*, 138–147. 10.1016/j.neuroimage.2017.10.020 (2018).

25 Jung R.E., & Haier R.J. The Parieto-Frontal Integration Theory (P-FIT) of intelligence: Converging neuroimaging evidence. *Behavioural and Brain Sciences.* **30**(2):154–187. 10.1017/S0140525X07001185 (2007)

26 Cox, S. R., Ritchie, S. J., Fawns-Ritchie, C., Tucker-Drob, E. M., & Deary, I. J. Structural brain imaging correlates of general intelligence in UK Biobank. *Intelligence*, *76*, 101376. 10.1016/j.intell.2019.101376 (2019).

27 Marek, S. et al. Reproducible brain-wide association studies require thousands of individuals. *Nature* **603,** 654–660 10.1038/s41586-022-04492-9 (2022).

28 Panizzon M.S. et al. Distinct genetic influences on cortical surface area and cortical thickness. *Cereb Cortex* 19:2728–2735 10.1093/cercor/bhp026 (2009).

29 Storsve A.B. et al. Differential longitudinal changes in cortical thickness, surface area and volume across the adult life span: regions of accelerating and decelerating change. *J Neurosci* 34:8488–8498, 10.1523/JNEUROSCI.0391-14.2014 (2014).

30 Dickerson B.C. et al. Differential effects of aging and Alzheimer's disease on medial temporal lobe cortical thickness and surface area. *Neurobiol Aging* 30:432–440 10.1016/j.neurobiolaging.2007.07.022 (2009).

31 Eyler L.T. et al. A comparison of heritability maps of cortical surface area and thickness and the influence of adjustment for whole brain measures: a magnetic resonance imaging twin study. *Twin Res Hum Genet* 15:304–314 10.1017/thg.2012.3 (2012).

32https://figshare.com/articles/dataset/A_FreeSurfer_view_of_the_cortical_transcriptome_generated_from_the_Allen_Human_Brain_Atlas/1439749

33 Kang, H., Kawasawa, Y., Cheng, F. et al. Spatio-temporal transcriptome of the human brain. Nature 478, 483–489 https://doi.org/10.1038/nature10523. (2011).

34 Sudlow, C. et al. UK biobank: an open access resource for identifying the causes of a wide range of complex diseases of middle and old age. *PLoS medicine*, *12*(3), e1001779. 10.1371/journal.pmed.1001779 (2015).

35 Habota, T. et al. Cohort profile for the STratifying Resilience and Depression Longitudinally (STRADL) study: A depression-focused investigation of Generation Scotland, using detailed clinical, cognitive, and neuroimaging assessments. *Wellcome open research*, *4*, 185. 10.12688/wellcomeopenres.15538.2 (2021).

36 Deary, I. J. et al. The Lothian Birth Cohort 1936: a study to examine influences on cognitive ageing from age 11 to age 70 and beyond. *BMC geriatrics*, *7*, 28. 10.1186/1471-2318-7-28 (2007).

37 Taylor, A. M., Pattie, A., & Deary, I. J. Cohort Profile Update: The Lothian Birth Cohorts of 1921 and 1936. *International journal of epidemiology*, *47*(4), 1042–1042r. 10.1093/ije/dyy022 (2018).

38 Miller, K. L. et al. Multimodal population brain imaging in the UK Biobank prospective epidemiological study. *Nature neuroscience*, *19*(11), 1523–1536. 10.1038/nn.4393 (2016).

39 Wardlaw, J. M. et al. Brain aging, cognition in youth and old age and vascular disease in the Lothian Birth Cohort 1936: rationale, design and methodology of the imaging protocol. *International journal of stroke : official journal of the International Stroke Society*, *6*(6), 547–559. 10.1111/j.1747-4949.2011.00683.x (2011).

40 Habota, T., Sandu, A. L., Waiter, G. D., et al. (2021). Cohort profile for the STratifying Resilience and Depression Longitudinally (STRADL) study: A depression-focused investigation of Generation Scotland, using detailed clinical, cognitive, and neuroimaging assessments. *Wellcome open research*, *4*, 185. https://doi.org/10.12688/wellcomeopenres.15538.2

41 Desikan, R. S. et al. An automated labeling system for subdividing the human cerebral cortex on MRI scans into gyral based regions of interest. *NeuroIm*age, *31*(3), 968–980. 10.1016/j.neuroimage.2006.01.021 (2006).

42 Fawns-Ritchie, C., & Deary, I. J. Reliability and validity of the UK Biobank cognitive tests. *PloS one*, *15*(4), e0231627. 10.1371/journal.pone.0231627 (2020).

43 Habota, T. et al. Cohort profile for the STratifying Resilience and Depression Longitudinally (STRADL) study: A depression-focused investigation of Generation Scotland, using detailed clinical, cognitive, and neuroimaging assessments. *Wellcome open research*, *4*, 185. 10.12688/wellcomeopenres.15538.2 (2021).

44 Ritchie, S. J. et al. Predictors of ageing related decline across multiple cognitive functions. *Intelligence*, *59*, 115–126. 10.1016/j.intell.2016.08.007 (2016).

45 Tucker-Drob, E. M., Briley, D. A., Starr, J. M., & Deary, I. J. Structure and correlates of cognitive aging in a narrow age cohort. *Psychology and aging*, *29*(2), 236–249. 10.1037/a0036187 (2014).

46 Ritchie, S. J. et al. Predictors of ageing related decline across multiple cognitive functions. *Intelligence*, *59*, 115–126. 10.1016/j.intell.2016.08.007 (2016).

47 Tucker-Drob, E. M., Briley, D. A., Starr, J. M., & Deary, I. J. Structure and correlates of cognitive aging in a narrow age cohort. *Psychology and aging*, *29*(2), 236–249. 10.1037/a0036187 (2014).

48 Revelle, W. *psych: Procedures for Psychological, Psychometric, and Personality Research*. Northwestern University, Evanston, Illinois. R package version 2.1.9, https://CRAN.R-project.org/package=psych. (2021).

49 Ogle, D.H., Dollm J.C., Wheeler, P., & Dinno, A. *FSA: Fisheries Stock Analysis*. R package version 0.9.1, https://github.com/droglenc/FSA. (2021).

50 Viechtbauer, W. "Conducting meta-analyses in R with the metafor package." *Journal of Statistical Software*, **36**(3), 1–48. 10.18637/jss.v036.i03. (2010).

51 Rosseel. Y. lavaan: An R Package for Structural Equation Modeling. *Journal of Statistical Software*, 48(2), 1-36. URL http://www.jstatsoft.org/v48/i02/. (2012).

52 Thomas, P. D., et al. PANTHER: a library of protein families and subfamilies indexed by function. *Genome research*, *13*(9), 2129–2141. 10.1101/gr.772403 (2003).

53 French, L., & Paus, T. A FreeSurfer view of the cortical transcriptome generated from the Allen Human Brain Atlas. *Frontiers in neuroscience*, *9*, 323. 10.3389/fnins.2015.00323 (2015).

54 Markello, R. D. et al. Standardizing workflows in imaging transcriptomics with the abagen toolbox. *eLife*, *10*, e72129. 10.7554/eLife.72129 (2021).

55 Markello, R., Shafiei, G., Zheng, Y. Q., Mišić, B. abagen: A toolbox for the Allen Brain Atlas genetics data. Available from: 10.5281/zenodo.5129257. (2021).

56 Kang, H., Kawasawa, Y., Cheng, F. et al. Spatio-temporal transcriptome of the human brain. Nature 478, 483–489 https://doi.org/10.1038/nature10523. (2011).

57 Wong, A. P. et al. Inter-Regional Variations in Gene Expression and Age-Related Cortical Thinning in the Adolescent Brain. *Cerebral cortex*, *28*(4), 1272–1281. 10.1093/cercor/bhx040 (2018).

58 French, L., & Paus, T. A FreeSurfer view of the cortical transcriptome generated from the Allen Human Brain Atlas. *Frontiers in neuroscience*, *9*, 323. 10.3389/fnins.2015.00323 (2015).

59 Yeo, B. T. et al. The organization of the human cerebral cortex estimated by intrinsic functional connectivity. *Journal of neurophysiology*, *106*(3), 1125–1165. 10.1152/jn.00338.2011 (2011).

60 Destrieux, C., Fischl, B., Dale, A., & Halgren, E. Automatic parcellation of human cortical gyri and sulci using standard anatomical nomenclature. *NeuroIm*age, *53*(1), 1–15. 10.1016/j.neuroimage.2010.06.010 (2010).

61 Thomas, P. D., et al. PANTHER: a library of protein families and subfamilies indexed by function. *Genome research*, *13*(9), 2129–2141. 10.1101/gr.772403 (2003).

62 Zeisel, A., et al. Brain structure. Cell-types in the mouse cortex and hippocampus revealed by single-cell RNA-seq. *Science, 347*(6226), 1138–1142. https://doi.org/10.1126/science.aaa1934 (2015).

63 Shin, J. et al. Cell-Specific Gene-Expression Profiles and Cortical Thickness in the Human Brain. *Cerebral cortex*, *28*(9), 3267–3277. 10.1093/cercor/bhx197 (2018).

64 O'Leary, N. A. et al. Reference sequence (RefSeq) database at NCBI: current status, taxonomic expansion, and functional annotation. *Nucleic acids research*, *44*(D1), D733–D745. https://doi.org/10.1093/nar/gkv1189 (2016).

65 Sudlow, C. et al. UK biobank: an open access resource for identifying the causes of a wide range of complex diseases of middle and old age. *PLoS medicine*, *12*(3), e1001779. 10.1371/journal.pmed.1001779 (2015).

66 Habota, T. et al. Cohort profile for the STratifying Resilience and Depression Longitudinally (STRADL) study: A depression-focused investigation of Generation Scotland, using detailed clinical, cognitive, and neuroimaging assessments. *Wellcome open research*, *4*, 185. 10.12688/wellcomeopenres.15538.2 (2021).

67 Deary, I. J. et al. The Lothian Birth Cohort 1936: a study to examine influences on cognitive ageing from age 11 to age 70 and beyond. *BMC geriatrics*, *7*, 28. 10.1186/1471-2318-7-28 (2007).

68 Taylor, A. M., Pattie, A., & Deary, I. J. Cohort Profile Update: The Lothian Birth Cohorts of 1921 and 1936. *International journal of epidemiology*, *47*(4), 1042–1042r. 10.1093/ije/dyy022 (2018).

69 Salthouse T. A. Relations between cognitive abilities and measures of executive functioning. *Neuropsychology*, *19*(4), 532–545. 10.1037/0894-4105.19.4.532 (2005).

70 Basten, U., Hilger, K., & Fiebach, C. J. Where smart brains are different: A quantitative meta-analysis of functional and structural brain imaging studies on intelligence. *Intelligence, 51,* 10–27. 10.1016/j.intell.2015.04.009 . (2015).

71 Peng, Z., Luo, Y., & Xiao, Z. Y. Angiopoietin-1 accelerates Alzheimer's disease via FOXA2/PEN2/APP pathway in APP/PS1 mice. *Life sciences*, *246*, 117430. 10.1016/j.lfs.2020.117430 (2020).

72 Kizuka, Y., Kitazume, S., Sato, K., & Taniguchi, N. Clec4g (LSECtin) interacts with BACE1 and suppresses Aβ generation. *FEBS letters*, *589*(13), 1418–1422. 10.1016/j.febslet.2015.04.060 (2015).

73 White, C. C. et al. Identification of genes associated with dissociation of cognitive performance and neuropathological burden: Multistep analysis of genetic, epigenetic, and transcriptional data. *PLoS medicine*, *14*(4), e1002287. 10.1371/journal.pmed.1002287 (2017).

74 Gns, H. S., Rajalekshmi, S. G., & Burri, R. R. Revelation of Pivotal Genes Pertinent to Alzheimer's Pathogenesis: A Methodical Evaluation of 32 GEO Datasets. *Journal of molecular neuroscience: MN*, *72*(2), 303–322. 10.1007/s12031-021-01919-2 (2022).

75 Xiao, M. F., et al. NPTX2 and cognitive dysfunction in Alzheimer's Disease. *eLife*, *6*, e23798. https://doi.org/10.7554/eLife.23798. (2017).

76 Shao, K., Shan, S., Ru, W., & Ma, C. Association between serum NPTX2 and cognitive function in patients with vascular dementia. *Brain and behavior*, *10*(10), e01779. https://doi.org/10.1002/brb3.1779. (2020).

77 Libiger, O. et al Longitudinal CSF proteomics identifies NPTX2 as a prognostic biomarker of Alzheimer's disease. *Alzheimer's & dementia : the journal of the Alzheimer's Association*, *17*(12), 1976–1987. https://doi.org/10.1002/alz.12353 (2021).

78 Belbin, O., et al. Cerebrospinal fluid profile of NPTX2 supports role of Alzheimer's disease-related inhibitory circuit dysfunction in adults with Down syndrome. *Molecular neurodegeneration*, *15*(1), 46. https://doi.org/10.1186/s13024-020-00398-0. (2020).

79 Gami-Patel, P. et al. The severity of behavioural symptoms in FTD is linked to the loss of GABRQ-expressing VENs and pyramidal neurons. *Neuropathology and applied neurobiology*, *48*(4), e12798. 10.1111/nan.12798 (2022).

80 Underwood, R. et al. The GTPase Rab27b regulates the release, autophagic clearance, and toxicity of α-synuclein. *The Journal of biological chemistry*, *295*(23), 8005–8016. 10.1074/jbc.RA120.013337 (2020).

81 Neumann, A. et al. Rare variants in IFFO1, DTNB, NLRC3 and SLC22A10 associate with Alzheimer's disease CSF profile of neuronal injury and inflammation. *Molecular psychiatry*, *27*(4). 10.1038/s41380-022-01437-6 (2022).

82 Zhu B. et al. The SEMA5A gene is associated with hippocampal volume, and their interaction is associated with performance on Raven's Progressive Matrices. *Neuroimage*. 88:181-7. 10.1016/j.neuroimage.2013.11.035. (2014).

83 Poke, G., Sadleir, L. G., Merla, G., de Valles-Ibáñez, G., & Skinner, J. R. *GNB5*-Related Neurodevelopmental Disorder. In M. P. Adam (Eds.) et. al., *GeneReviews*®. University of Washington, Seattle. (2021).

84 Lodder, E. M. et al. GNB5 Mutations Cause an Autosomal-Recessive Multisystem Syndrome with Sinus Bradycardia and Cognitive Disability. *American journal of human genetics*, *99*(3), 786. 10.1016/j.ajhg.2016.08.011 (2016).

85 Shibata, M. et al. Regulation of prefrontal patterning and connectivity by retinoic acid. *Nature*, *598*(7881), 483–488. 10.1038/s41586-021-03953-x (2021).

86 Wołoszynowska-Fraser, M. U., Rossi, S. L., Long, J. M., McCaffery, P. J., & Rapp, P. R. Differential Retinoic Acid Signaling in the Hippocampus of Aged Rats with and without Memory Impairment. *eNeuro*, *8*(5), 10.1523/ENEURO.0120-21.2021 (2021).

87 Blundell, J., Hoang, C. V., Potts, B., Gold, S. J., & Powell, C. M. Motor coordination deficits in mice lacking RGS9. *Brain research*, *1190*, 78–85. 10.1016/j.brainres.2007.11.017 (2008).

88 Hattori, K. et al. Blood CADPS2ΔExon3 expression is associated with intelligence and memory in healthy adults. *Biological psychology*, *89*(1), 117–122. 10.1016/j.biopsycho.2011.09.017 (2012).

89 Jablensky, A. et al. Promoter polymorphisms in two overlapping 6p25 genes implicate mitochondrial proteins in cognitive deficit in schizophrenia. *Molecular psychiatry*, *17*(12), 1328–1339. 10.1038/mp.2011.129 (2012).

90 Pineda-Cirera, L., Cabana-Domínguez, J., Lee, P. H., Fernàndez-Castillo, N., & Cormand, B. Identification of genetic variants influencing methylation in brain with pleiotropic effects on psychiatric disorders. *Progress in neuro-psychopharmacology & biological psychiatry*, *113*, 110454. 10.1016/j.pnpbp.2021.110454 (2022).

91 Markello RD, et al. Standardizing workflows in imaging transcriptomics with the abagen toolbox. Elife. 10:e72129. doi: 10.7554/eLife.72129. (2021).

92 Buchanan, C. R. et al. Comparison of structural MRI brain measures between 1.5 and 3 T: Data from the Lothian Birth Cohort 1936. *Human Brain Mapping*, 42(12), 3905– 3921. 10.1002/hbm.25473 (2021).

93 Nikolaidis, A. et al. Suboptimal phenotypic reliability impedes reproducible human neuroscience. bioRxiv 2022.07.22.501193; doi: https://doi.org/10.1101/2022.07.22.501193